Supporting Information

Latimer et al. 10.1073/pnas.1404477111

SI Materials and Methods

Animals and Vitamin D Diets. Sixty middle-aged (11–13 mo old) male F344 rats from the National Institute on Aging aging rodent colony were housed two to a cage and maintained on ad libitum food and water. All protocols were approved by the Institutional Animal Care and Use Committee of the University of Kentucky. Animals were divided into three groups, each receiving a different dietary amount of cholecalciferol [vitamin D3 (VitD3)]. VitD3, the precursor of 25-hydroxyvitamin D (25OHD), is typically derived from exposure to sunlight, fortified foods, or supplements (1). A purified AIN-93 (Harlan–Teklad) diet was modified to contain low, medium (National Research Council-required), or high VitD3 (2) (Table 1). Animal weights (Fig. S1) and food intake were measured two to three times per week. The average daily intake of VitD3 was calculated based on the amount of VitD3 in each diet and the average food intake (Table 1).

To monitor general health and reduce potential confounding effects of stress, animals were handled throughout the study. Seven rats were removed from the study. Two were euthanized for health reasons: One high-VitD3 rat lost significant weight, and a low-VitD3 rat developed a large lipoma. Two rats each from the low-VitD3 and high-VitD3 groups were removed due to a change from paired to single housing, an environmental change that could affect behavior. Another high-VitD3 rat was removed because it showed persistent unusual behavior and never adapted to handling. All of the 53 remaining rats exhibited normal behaviors, such as grooming, curiosity, and mobility.

Morris Water Maze. The Morris water maze (MWM) procedures were similar to MWM procedures previously described (3). To assess learning, animals were trained for 3 consecutive days, three trials per day, to find the submerged platform. Twenty-four hours after the last training day, the platform was removed and the probe trial was conducted to assess memory. The next day, the platform was moved to another quadrant and animals were given three trials to learn the new location (reversal learning). Seventy-two hours later, another probe trial (reversal probe) was conducted, followed by visual cue assessment on the final day (Fig. 3*A*). For the visual cue, the platform was indicated by a white cup hanging over the platform. All rats performed optimally on the visual cue, indicating that group differences in maze performance could not be attributed to visual impairment. Maze performance was evaluated by measuring path length and latency to detection of the submerged platform.

Tissue Preparation. Two weeks after completing the MWM, rats were deeply anesthetized (100 mg/kg of pentobarbital administered i.p.) and blood was collected from the right ventricle immediately before a 10-min intracardial perfusion with ice-cold saline (peristaltic pump at 13 mL/min). Brains were then rapidly removed and hemisected. The right hemisphere was placed in 4% paraformaldehyde for overnight fixation and used for immunohistochemistry (IHC; discussed below). The hippocampus of the left hemisphere was dissected and stored in an RNase-free tube at −80 °C for subsequent microarray analyses.

Blood levels of 25OHD were determined by LC-tandem MS. Blood samples were spotted onto ZRT filter paper cards, dried at room temperature for 30 min, and shipped to ZRT Laboratory for analysis. Isolated serum samples were shipped to the Research Animal Diagnostic Laboratory at the University of Missouri (IDEXX RADIL) for blood chemistry panel analysis (Table S1).

Microarrays. Microarray procedures and analyses were performed as in prior work (4). Briefly, hippocampal RNA was isolated, quantified, and checked for RNA integrity. One low-VitD3 sample failed RNA quality control. The remaining RNA samples were applied to Affymetrix Rat Gene 1.0 ST arrays (one array per subject). Prestatistical filtering removed poorly annotated probe sets, low-intensity signals, and outlier values (>2 SD of the group mean). Filtered data were analyzed by one-way ANOVA to identify significant differences, and the false discovery rate procedure (5) was used to estimate the error of multiple testing. Significant genes were assigned to one of four idealized expression patterns using Pearson's test and were separated by the sign of their correlation; expression values for probe set intensities are represented as log-2 values (Dataset S1). Functional categorization for significant genes was determined using the Database for Annotation, Visualization, and Integrated Discovery (DAVID) suite of bioinformatic tools (6, 7) (Table 2). The results of the study have been uploaded to the Gene Expression Omnibus (www.ncbi.nlm.nih.gov/geo/).

Vitamin D Response Element Identification. Identification of significant genes that contain a potential vitamin D response (VDR) element was performed using Partek Genomics software. Because the VDR heterodimerizes with the retinoid-X receptor (RXR) before DNA binding, the relevant motif consists of both a 6-bp binding site for RXR and a 6-bp binding site for VDR, separated by three random base pairs (5′GGGTCA-NNN-GGTTCA3′). The rat genome was searched for sequences within the promoter regions of the significant genes that were at least 70% homologous with this motif.

IHC. Right hemispheres were removed from overnight fixation, transferred to 30% sucrose, and cut on a microtome into 30-μm coronal sections. Tissue was transferred to a blocking buffer (10% horse serum/0.05 M Tris buffer with 0.5% Triton X-100) for 1 h. Sections were then placed in primary antibody solution with blocking buffer for 2–3 d on a shaking table at 4 °C [Ab4707–anti-VDR goat polyclonal (1:8,000; courtesy of Nicholas Koszewski, Iowa State University, Ames, IA) (8, 9); regarding the specificity of Ab4707 for VDR, Langub et al. (9) have shown negligible staining in liver, which lacks VDR (10, 11); Ab24591–anti-synaptojanin mouse monoclonal (1:4,000; Abcam); and znp-1–anti-synaptotagmin mouse monoclonal (1:8,000; ZIRC)]. After incubation, sections were rinsed three times in 0.05 M Tris and transferred to the secondary antibody [donkey anti-goat or anti-mouse biotin (1:800; Jackson ImmunoResearch)] for 1 h and rinsed three times in 0.05 M Tris. Sections were then transferred to a peroxidase-conjugated streptavidin solution (1:1,000; Jackson ImmunoResearch) for 1 h, rinsed three times in 0.05 M Tris, and then incubated for 20 min with nickel-enhanced diaminobenzidine. Digitized images of stained sections were obtained using a Nikon Eclipse 90i microscope and a Nikon DS-Ri1 camera. All images were acquired in a single session with the same camera settings. Staining intensity (optical density) was assessed on raw images for VDR, synaptojanin 1, and synaptotagmin 2 (Nikon Elements Basic Research analysis software).

Hipppocampal Slice Electrophysiology. Electrophysiological analyses were performed on isolated hippocampal slices from the remaining rats (those rats not designated for microarrays and IHC, see Fig. 1). Because practical constraints limited recording to a single rat per day, recordings were obtained over the course of 5 wk after the MWM test. During this time, rats were maintained on their respective VitD3-containing diets. Hippocampal slices were obtained, and

long-term potentiation (LTP) was recorded as previously described (3). Briefly, a stimulating electrode was placed in the stratum radiatum, and extracellular field excitatory postsynaptic potentials (fEPSPs) were recorded in the CA1 region. Input/output (I/O) characteristics were examined by recording fEPSPs in the CA1 resulting from stimuli of increasing intensity. The stimulation intensity was set at 33% of the maximum response, as determined from the I/O curve. Following 20 min of baseline recordings, LTP was induced (2-s theta-burst, eight pulses at 100 Hz, 50 ms each, at 5 Hz) and post-LTP recordings were obtained for 30 min.

Statistics. Food intake, blood chemistry, and behavior and electrophysiology data were analyzed by one-way ANOVA with a Newman–Keuls multiple comparison post hoc test. A Grubbs test was run to identify outliers. Semiquantitative IHC density data were averaged across three sections to create a single measure per animal. Because gene expression of synaptojanin 1 and synaptotagmin 2 did not differ between the low- and medium-VitD3 groups, they were analyzed as a single group for IHC analysis and compared with the high-VitD3 group using a t test. For all analyses, statistical significance was defined as $P \leq 0.05$.

1. Holick MF (2007) Vitamin D deficiency. *N Engl J Med* 357(3):266–281.
2. Fleet JC, et al. (2008) Serum metabolite profiles and target tissue gene expression define the effect of cholecalciferol intake on calcium metabolism in rats and mice. *J Nutr* 138(6):1114–1120.
3. Blalock EM, et al. (2010) Effects of long-term pioglitazone treatment on peripheral and central markers of aging. *PLoS ONE* 5(4):e10405.
4. Kadish I, et al. (2009) Hippocampal and cognitive aging across the lifespan: A bioenergetic shift precedes and increased cholesterol trafficking parallels memory impairment. *J Neurosci* 29(6):1805–1816.
5. Hochberg Y, Benjamini Y (1990) More powerful procedures for multiple significance testing. *Stat Med* 9(7):811–818.
6. Huang W, Sherman BT, Lempicki RA (2009) Systematic and integrative analysis of large gene lists using DAVID bioinformatics resources. *Nat Protoc* 4(1):44–57.
7. Gene Ontology Consortium (2010) The Gene Ontology in 2010: Extensions and refinements. *Nucleic Acids Res* 38(Database issue):D331–D335.
8. Brewer LD, et al. (2001) Vitamin D hormone confers neuroprotection in parallel with downregulation of L-type calcium channel expression in hippocampal neurons. *J Neurosci* 21(1):98–108.
9. Langub MC, Reinhardt TA, Horst RL, Malluche HH, Koszewski NJ (2000) Characterization of vitamin D receptor immunoreactivity in human bone cells. *Bone* 27(3): 383–387.
10. Wang Y, Becklund BR, DeLuca HF (2010) Identification of a highly specific and versatile vitamin D receptor antibody. *Arch Biochem Biophys* 494(2):166–177.
11. Wang Y, Zhu J, DeLuca HF (2012) Where is the vitamin D receptor? *Arch Biochem Biophys* 523(1):123–133.

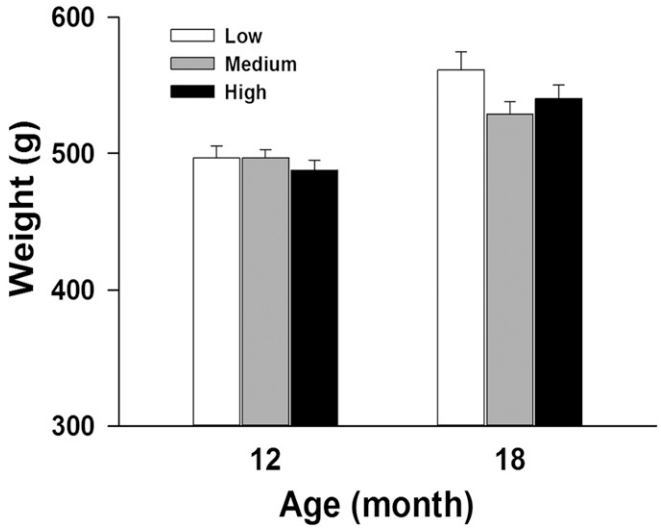

Fig. S1. Body weights of male F344 rats on different VitD3 diets over the course of the study. At the beginning, animals ranged in age from 11 to 13 mo; thus, the ages indicated above reflect the mean age for all rats. Animals in each group showed a significant age-related increase in body weight (paired t test, $P = 0.001$; $n = 16–20$ per group). Low-VitD3 animals gained the most weight over time, but this weight gain was not significantly different from the age-related weight gain seen in the medium- or high-VitD3 groups.

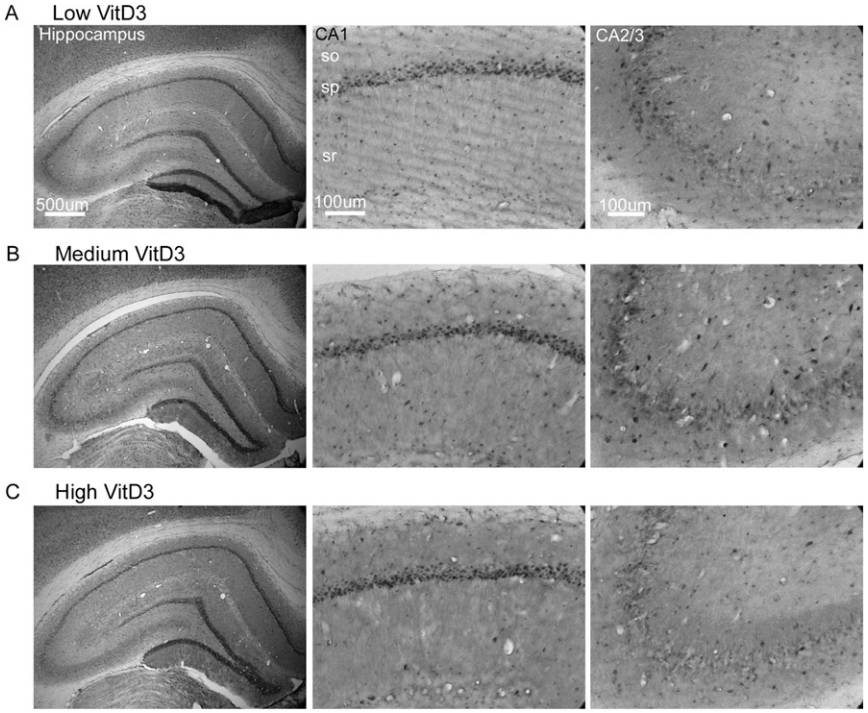

Fig. S2. Representative images of VDR immunoreactivity in the hippocampus of VitD3-treated animals. VDR immunoreactivity was detected in the hippocampus of rats treated with low (*A*), medium (*B*), and high (*C*) VitD3. No apparent differences in VDR expression or distribution were detected between groups. Specifically, VDR immunoreactivity was seen in the neuronal cell body layers of both the CA1 and CA2/3 regions of the hippocampus, as well as in the dentate gyrus. Some more diffuse staining is also observed in other hippocampal areas (so, stratum oriens; sp, stratum pyramidale; sr, stratum radiatum). Regarding the specificity of Ab4707 for VDR, Langub et al. (9) have shown negligible staining in liver, which lacks VDR (10, 11).

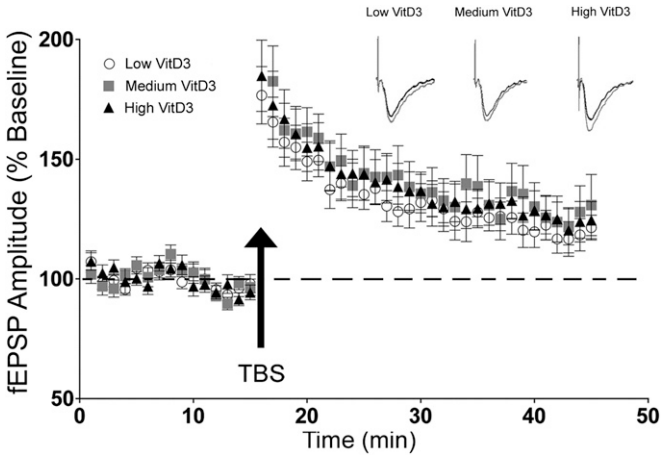

Fig. S3. Theta burst-induced synaptic potentiation recorded from the CA1 region of the hippocampus of VitD3-treated rats. Normalized EPSP slopes were measured across all treatment groups during baseline and following theta burst stimulation (TBS). No differences were observed between groups. After baseline recordings, LTP was induced using a 2-s tetanizing TBS pattern, consisting of eight pulses at 100 Hz (50 ms each), delivered at 5 Hz in the stratum radiatum. Stimulus intensity was set at 33% of the maximum response, which was determined from the I/O curve (Fig. 5) before LTP induction. Following the TBS, fEPSP responses were obtained for 30 min using the same stimulus protocol as the baseline pattern. (*Insets*) Representative averaged EPSP traces for each group are shown. Data represent mean ± SEM from 16 to 22 hippocampal slices from seven to nine animals per group.

Table S1. Blood serum chemistry panel

Blood chemistry variables	Low VitD3	Medium VitD3	High VitD3
Calcium, mg/dL	11.3 ± 0.1	11.3 ± 0.10	11.5 ± 0.1
Phosphorus, mg/dL	5.6 ± 0.2	4.9 ± 0.2	5.4 ± 0.1
Magnesium, mg/dL	2.7 ± 0.1	2.6 ± 0.1	2.7 ± 0.1
Iron, μg/dL	207.1 ± 12.6	211.8 ± 7.1	213.7 ± 9.1
Blood urea nitrogen, mg/dL	17.2 ± 0.7	17.1 ± 0.9	19.4 ± 3.1
Creatinine, mg/dL	0.6 ± 0.02	0.59 ± 0.04	0.64 ± 0.06
Sodium, mmol/L	142.4 ± 0.2	141.8 ± 0.8	142.2 ± 0.3
Potassium, mmol/L	4.2 ± 0.2	4.0 ± 0.1	4.2 ± 0.1
Chloride, mmol/L	97.0 ± 0.4	96.9 ± 0.7	97.1 ± 0.3
Total protein, g/dL	7.30 ± 0.08	7.28 ± 0.10	7.32 ± 0.13
Albumin, g/dL	3.5 ± 0.1	3.5 ± 0.1	3.5 ± 0.1
Total bilirubin, mg/dL	0.13 ± 0.02	0.16 ± 0.02	0.17 ± 0.02
ALT, U/L	64.6 ± 6.1	57.8 ± 7.0	52.1 ± 5.4
ALP, U/L	97.8 ± 5.7*	125.2 ± 8.2	111.9 ± 4.9
GGT, U/L	<3	<3	<3
LDH, U/L	400.7 ± 27.6	404.4 ± 37.1	388.4 ± 42.2
Glucose, mg/dL	151.5 ± 12.4	179.3 ± 12.2	173.6 ± 6.7
HbA1C	3.3 ± 0.1	3.3 ± 0.1	3.3 ± 0.0
Triglycerides, mg/dL	188.2 ± 33.7	222.6 ± 26.3	256.7 ± 42.1
Cholesterol, mg/dL	198.7 ± 22.1	186.3 ± 5.2	210.7 ± 17.7
Total CO_2, mmol/L	22.3 ± 0.5	24.3 ± 0.4	22.7 ± 0.6

ALP, alkaline phosphatase; ALT, alanine aminotransferase; GGT, gamma-glutamyl transpeptidase; HbA1C, glycated hemoglobin; LDH, lactate dehydrogenase. *$P < 0.05$, different from medium VitD3.

Other Supporting Information Files

Dataset S1 (XLSX)